Ceramics International **22** (1996) 335–340

0272-8842(95)00115-8
0272-8842/96/$15.00

Titanium Implantation into Boron Nitride Films and Ion-Beam Mixing of Titanium–Boron Nitride Multilayers

Wolfram Gissler & Peter Neil Gibson

Institute for Advanced Materials, Joint Research Centre of the Commission of the European Communities, Ispra (Va), Italy

(Received 22 July 1995; accepted 2 September 1995)

Abstract: Ti–B–N films of various composition and crystalline structure have been synthesized by titanium ion implantation into sub-stoichiometric and stoichiometric hexagonal boron nitride films. Due to the relatively low penetration depth of Ti^+ ions these films can only be prepared with limited thickness, of the order of several hundred nanometers. Ti–B–N films were also prepared by ion-beam mixing of multilayer coatings of the sequence Ti/BN by argon ion bombardment. With these methods, inhomogeneous coatings with respect to their composition, in particular at low fluences, were obtained. All films were investigated by glancing angle X-ray diffraction. SEM, SNMS and ESCA/Auger analysis were also performed on some of the samples. Hardness and Young's modulus were determined by an ultra-low load, depth-sensing nanoindenter. Most of the results can be understood by examination of the chemical composition and crystalline structure of the films.

1 INTRODUCTION

The interest in titanium boron nitride coatings is due to their outstanding properties, such as ultra-high hardness in combination with high toughness, high temperature stability, good wear and corrosion resistance. These properties originate to a great part from the fact that this material exists in the form of a two or multiphase system.[1] No ternary compounds are known. Multiphase systems may offer considerable advantages over single phase systems since they often display better material properties than would be expected simply from the properties of the single phases of which they are composed.[2,3] By a suitable choice of combination of phases it is even possible to optimize properties such as hardness and toughness.[4] To do this it is necessary to synthesize the coatings with a well defined stoichiometry which is not possible with many of the deposition techniques currently in use. Ion implantation and ion-beam mixing are methods which offer in this respect a high degree of flexibility.

Up to the present, Ti–B–N films have been prepared by CVD,[5] PACVD,[6,7] arc PVD[8,9] and sputtering.[10–13] Several other methods have been applied, such as interdiffusion of Ti/BN multilayer films,[14] co-sputtering from Ti and BN targets[15,16] and sputtering from a heterogeneous Ti/BN target.[17] Recently the first results of Ti^+ implantation into $BN_{0.5}$ and BN layers were reported, as well as of ion-beam mixing of Ti/BN multilayers.[18,19]

In this paper the preparation of Ti–B–N films by Ti^+ ion implantation into h-BN films and by ion-beam mixing with multilayers of the sequence Ti/BN will be treated in more detail. The films were investigated by SEM, glancing angle X-ray diffraction (GAXRD), SNMS, ESCA/Auger analysis and nanoindentation.

2 EXPERIMENTAL

Boron nitride and titanium films were magnetron sputter deposited in a commercially available sputtering machine (MRC, type 8667A) in a pure Ar atmosphere from h-BN or Ti targets. Both targets were of a purity better than 97.5 at%. The diameter was 21 cm and the distance from the target to the substrate holder was 9 cm. An Ar flow of 50 sccm was maintained during deposition giving a total pressure of 0.5 Pa. The partial pressure of

the working and residual gas was measured by a quadrupole gas analyser, which was connected to the sputter chamber by a pressure converter. Gas contaminations were of the order of 0.3%. Evacuation to 5×10^{-5} Pa was accomplished by a 3000 litre/s cryogenic pumping system. Prior to deposition the targets were sputter-cleaned for approximately 20 min.

BN films were deposited on to polished silicon (111) wafers and Ti/BN multilayers on to glass substrates. Cleaning was performed with trichlorethylene and isopropanol in an ultrasonic bath, and before sputter deposition the substrates were subjected to a sputter etch for about 1 min.

Multilayer films were deposited positioning the substrate holder sequentially under the Ti and the BN targets. The sputter power was 300 W at the titanium target and 1 kW at the BN target. The time under the target was chosen according to the desired thickness of each layer. The thickness of the BN films was between 200 and 300 nm. Sub-stoichiometric films of composition $BN_{0.5}$ and stoichiometric BN films were used. The multilayers consisted of five bilayers of 20 nm of Ti and 8 nm of BN, with an extra layer of Ti at the glass interface.

Ion implantations were performed using a variable source high current implanter (Danfisik 1090) at an energy of 200 keV at low current (100 μA) in order to maintain the samples at low temperatures. Various fluences were used ranging from 5×10^{16} to 3×10^{18} ions/cm^2 for Ti implantation into BN films, and from 1×10^{15} to 1×10^{17} ions/cm^2 for Ar^+ ion-beam mixing of the multilayers.

X-ray microstructural analysis of the samples was performed with the glancing angle X-ray diffraction (GAXRD) apparatus described previously,[22] using CuK_α radiation. The angle of incidence of the incident beam on the sample surface was 0.5°, which results in theoretical penetration depths of about 5.5 μm in boron nitride and 0.5 μm in titanium, titanium nitride and titanium diboride.

The composition of the coatings was investigated by ESCA-Auger spectroscopy with a Perkin Elmer spectrometer type ESCA-SAM. The elemental concentrations were determined from the areas under the Ti 2p, N 1s and B 1s peaks, respectively, using atomic sensitivity factors. SNMS depth profiles were obtained with a Leybold INA3 machine.

Hardness and Young's modulus were determined by an ultra-low load depth-sensing nanoindenter (Nanoindonter II, from Nano Instruments Inc.) from the loading and unloading curves.[20] The loading curve was measured three times by keeping the indentation rate constant (3 nm/s) and measuring the displacement until a total depth of 50, 100 and 200 nm was reached. A hold period of 180 s followed, to allow for a relaxation of the induced plastic flow. Finally the unloading curve was measured, decreasing the force at a constant rate of about 40 μN/s. Elastic contributions were determined from the unloading curve. These were used for the calculation of Young's modulus and to reduce the loading curve to its plastic component alone. The measurements were calibrated with a Si (111) wafer assuming a modulus of 157 GPa, independent of penetration depth. Under these conditions a penetration depth independent hardness of 12 GPa was obtained for the Si wafer.

3 RESULTS

SEM images were taken of the surfaces of selected Ti implanted BN films in order to observe any macroscopic effects of the implantation. Two such images are presented in Fig. 1, one of a BN film implanted with a fluence of 1×10^{18} Ti^+/cm^2,

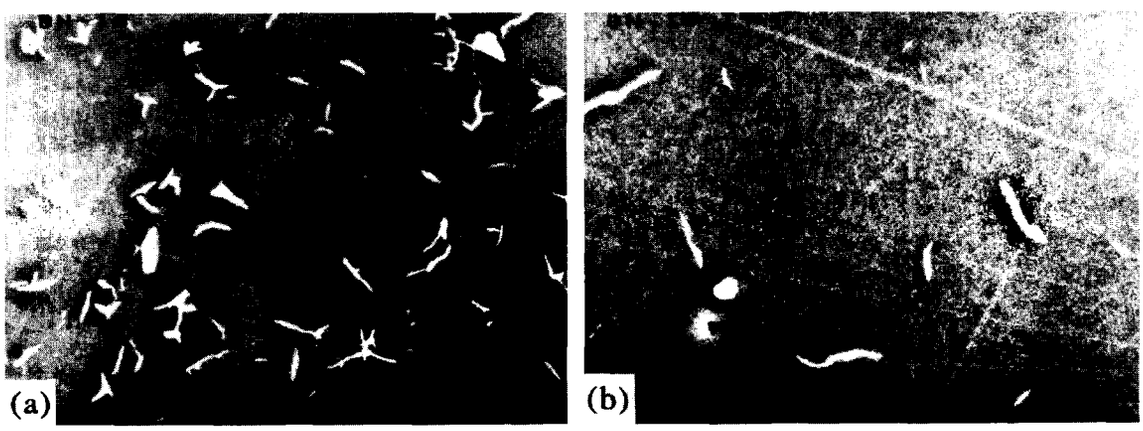

Fig. 1. SEM micrographs of (a) a BN film implanted with a fluence of 1×10^{18} Ti^+/cm^2 and (b) of the same film following annealing for 3 h at 500°C.

and the other of the same film following a post-implantation annealing for 3 h at 500°C. The surface of the implanted film displays many crack-like features of the order of 10 μm in size. We believe that this is probably stress-related cracking caused by a change in the density of the surface during the formation of new phases. Following the annealing treatment a "self-healing" effect becomes evident (Fig. 1(b)), the cracks reducing in size with time of annealing. This is probably due to atomic diffusion at the higher temperature, and related recrystallization. The depth profiles of the various atomic constituents of as-deposited and ion-implanted BN films, as well as of unimplanted and implanted Ti/BN multilayers, were investigated either by the SNMS or Auger techniques. Figure 2 shows the SNMS profiles of an as-deposited BN film (a), and of an identical film following implantation with 1×10^{18} Ti^+/cm^2 (b). The profiles (logarithmic scale) display a full width at half maximum, which is nearly extended over the whole BN film. Figure 3 shows Auger depth profiles of two Ti/BN multilayers, one unimplanted and the other ion-beam mixed with 10^{16} Ar^+/cm^2. Due to the depth resolution of the Auger technique it is difficult to follow subtle changes at the Ti/BN interfaces. A definite smearing of the interfaces is however apparent in the mixed specimen. Due to the interference of the Ti 2p and N 1s lines it is difficult to determine the relative concentration of N in the depth profile.

The structure of all unimplanted and implanted specimens was examined using GAXRD. This technique is much more surface-sensitive than standard XRD; however it should be noted that only those phases containing Ti are detectable in the cases under consideration here due to the weak scattering power of B and N. Figure 4 shows the GAXRD spectra of $BN_{0.5}$ films implanted with fluences of 1×10^{17}, 3×10^{17}, 1×10^{18} and 3×10^{18} Ti^+/cm^2. The width of all the diffraction peaks is large indicating that the implanted region is comprised of one or more nanocrystalline phases. The peaks have been identified as shown in the figure.

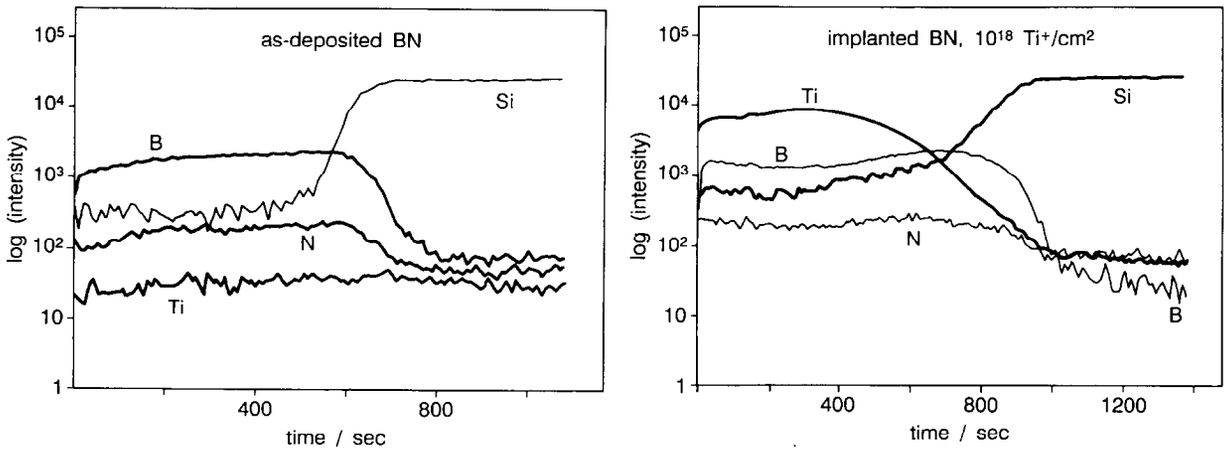

Fig. 2. SNMS profiles of (a) an as-deposited BN film, and (b) an identical film following implantation with 1×10^{18} Ti^+/cm^2.

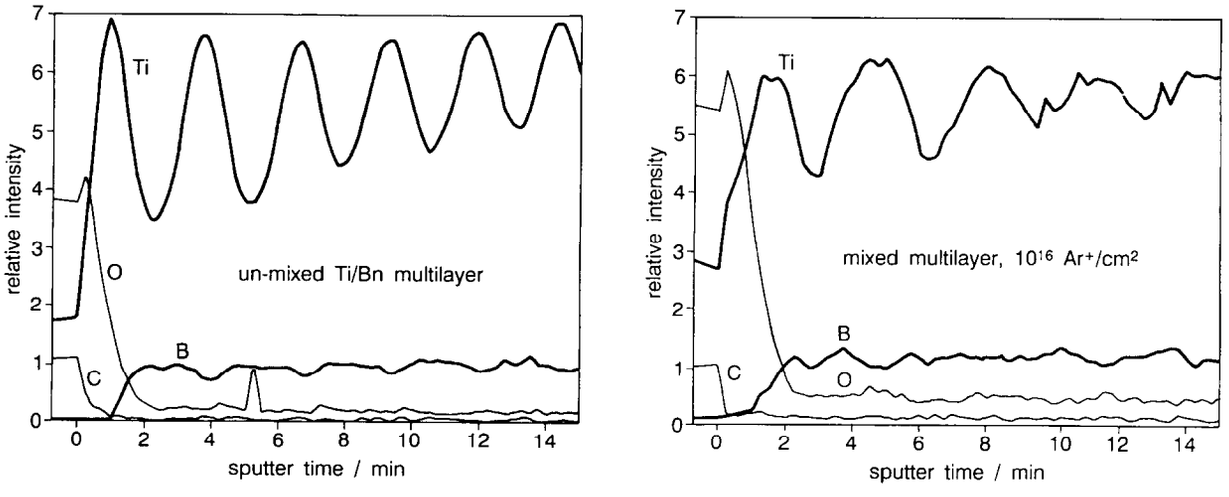

Fig. 3. Auger depth profiles of (a) an unimplanted Ti/BN multilayer, and (b) a Ti/BN multilayer ion-beam mixed with 10^{16} Ar^+/cm^2.

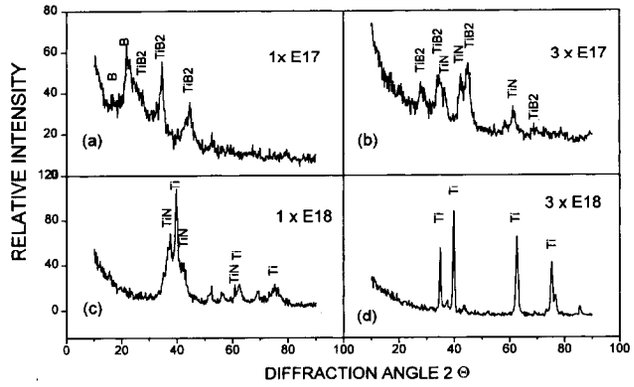

Fig. 4. GAXRD spectra of $BN_{0.5}$ films implanted with various fluences of Ti^+ ions.

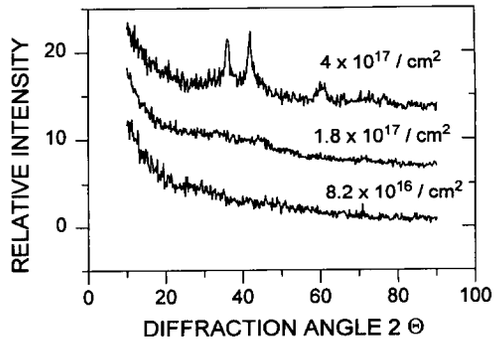

Fig. 5. GAXRD spectra of stoichiometric BN implanted with various fluences of Ti^+ ions.

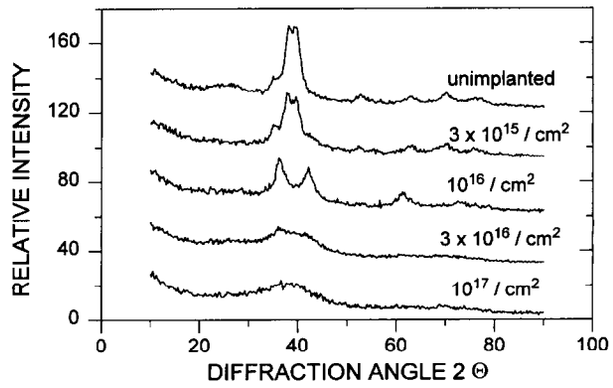

Fig. 6. GAXRD spectra of Ti/BN multilayers mixed by various Ar^+ ion fluences.

Figure 5 shows the GAXRD spectra of stoichiometric BN films, implanted with fluences of 8.2×10^{16}, 1.8×10^{17} and 4×10^{17} Ti^+/cm^2. The obvious difference between these sets of spectra is the lack of TiB_2 peaks in the spectra of the implanted stoichiometric BN films.

The spectra of ion-beam mixed Ti/BN multilayers after various ion fluences are shown in Fig. 6. The spectrum of the unmixed sample shows only the Ti peaks as expected. The broad scattering feature near $2\theta \approx 26°$ is probably due to penetration of some of the X-rays through to the glass substrate. After 10^{15} ions/cm^2 no obvious new phase has formed (spectrum not shown), while implantation with 3×10^{15} ions/cm^2 causes a change in shape of the main group of peaks near $2\theta \approx 40°$, indicating the possible formation of a second Ti-containing phase. The structure of this phase is immediately obvious following 10^{16} ions/cm^2 where it appears that practically all of the metallic Ti phase has disappeared in order to form a TiN phase. Further ion implantation rapidly destroys this phase, leaving an amorphous surface presumably containing Ti, N and B with some residual Ar.

Additional structural information was obtained from XPS measurements. These showed that for the $BN_{0.5}$ coatings implanted with a fluence of 1×10^{18} and 3×10^{17} Ti^+/cm^2 (Fig. 4) the Ti $2p_{3/2}$ line is split into two components at approximately 454.3 and 455.2 eV indicative of TiB_2 and TiN, respectively, showing that Ti is present in two different phases.

Hardness, H, and Young's modulus, E, of as-deposited $BN_{0.5}$ coatings and coatings which were annealed for 4 h at 400°C are shown in Fig. 7 as a function of the Ti^+ fluence.[19] In the figure curves obtained at different penetration depths are displayed. These all show a similar form, indicating that the films are rather homogeneous in chemical and phase composition. H and E obtained from the Ti^+-implanted stoichiometric BN films and from the mixed multilayer films are displayed in Figs 8 and 9, respectively.

4 DISCUSSION

Figure 10 shows a simplified phase diagram of the system Ti–B–N at 1500°C.[1] Two features have to be noted: (i) no ternary phases occur, and (ii) there is only a small boron solubility in titanium nitrides and a negligibly small solubility of nitrogen in the titanium boride phases. The crystal structures of the phases are the hexagonal AlB_2-type for the TiB_2 phase, the NaCl-type for the TiN, $TiN_{(1-x)}$ and $Ti(BN)_{1-x}$ phases, the orthorhombic, FeB-type for the TiB phase and the Mg-type for the Ti and phases and their solid solutions. The stable crystalline structure of boron nitride is a graphite-type structure.

The points plotted in Fig. 10 represent the average composition of the coatings prepared by Ti^+ implantation into $BN_{0.5}$ (open circles) and stoichiometric BN films (filled circles) as calculated from the Ti^+ fluence and thickness of the film assuming that all impinging Ti^+ ions remain in the film (projected range for 200 keV Ti^+ ions in BN

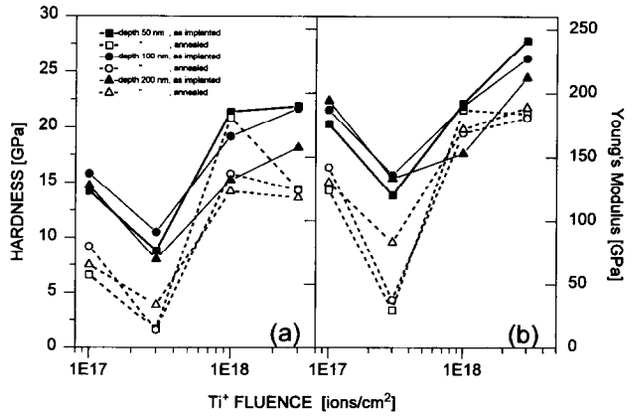

Fig. 7. Hardness and Young's modulus of Ti^+-implanted $BN_{0.5}$ films measured with a nanoindenter at various penetration depths.

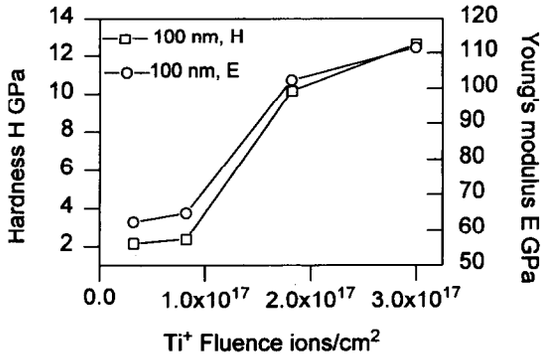

Fig. 8. Hardness and Young's modulus of a Ti^+-implanted stoichiometric BN film.

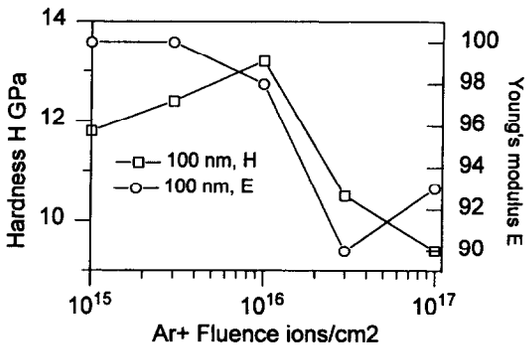

Fig. 9. Hardness and Young's modulus of Ar^+-mixed Ti/BN multilayers.

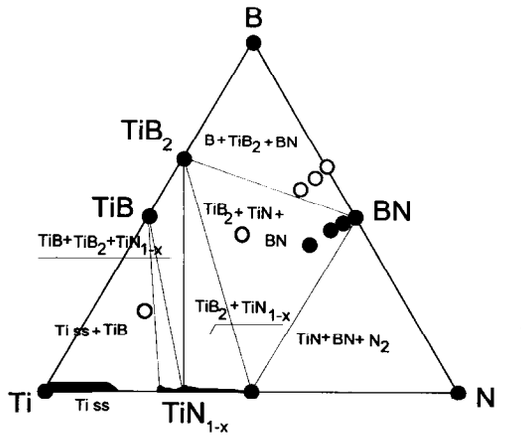

Fig. 10. Phase diagram (simplified) of the Ti–B–N system. The compositional locations of the implanted films are shown by open circles ($BN_{0.5}$) and filled circles (stoichiometric BN).

$\approx$ 170 nm). Due to the relatively flat Ti^+ implantation profile (Fig. 2) the local deviations from the average value should be within $\pm$ 30%.

In spite of the limited validity of phase diagrams for coatings deposited under "non-equilibrium" conditions, the experimentally identified phases are in good agreement with the phase diagram for the Ti–B–N system: only binary phases were observed (TiB_2 and TiN) and the evolution of the phase composition with implantation fluence (Figs 4 and 5) can be roughly described by

$$h - BN \rightarrow TiB_2, TiN \rightarrow Ti, TiN, TiB_2$$

as expected for the compositions corresponding to the different film compositions plotted in Fig. 10. The difference in the GAXRD spectra of Figs 4 and 5 for nearly equal fluences of 3×10^{17} and 4×10^{17} Ti^+/cm^2 can easily be understood from the different nitrogen concentrations in the films: both films are located in that zone of the phase diagram where the TiB_2, TiN and BN phases coexist. However, the stoichiometric film is expected to have at equal Ti^+ fluence a higher TiN phase fraction, since the free enthalpy of formation of TiN is a factor of 1.5 more negative than that for TiB_2.

Concerning the ion-beam mixed multilayer films it is not possible to attribute to them an approximate film composition as we have done for the implanted BN films. This is due to the fact that ion-beam mixing gives only at very high fluences (which could not be realized in our experiments) a sufficiently homogeneous mixing. Nevertheless, it is interesting to note that the films become highly X-ray amorphous at fluences above 3×10^{16} Ar^+/cm^2 (Fig. 6) in contrast to the implanted BN films at comparable fluences (see Figs 4 and 5). This behaviour is possibly a consequence of an accumulation of Ar^+ ions in the film. These may introduce high compressive stress and crystal disorder and lead to an effective decrease of crystallite size.

The observed dependence of hardness and Young's modulus (Figs 7–9) can also be qualitatively understood from the phase diagram. The hardest phases in the system are TiB_2 (H_v 4000) and TiN (H_v 2500). Higher hardness, and possibly

also higher toughness, might be obtained if the films have a multi-phase composition[2,3] with the restrictive condition that soft phases such as h-BN and Ti should be absent. These conditions are fulfilled if the chemical composition corresponds approximately to $TiBN_{0.5}$.[4] In this case the coating is composed only of the two hard phases TiB_2 and TiN in equal parts. The experimental results displayed in Fig. 7 confirm these expectations: highest hardness is actually observed at a fluence of about 1×10^{18} Ti^+/cm^2 (for the post-annealed films) corresponding to a composition of $TiBN_{0.5}$. However, only relatively moderate values for H and E of about 20 and 200 GPa were observed in comparison to about 50 and 500 GPa for Ti–B–N coatings which were synthesized by other methods.[15,16] The softening observed at very high fluences of Ti^+ implantation into $BN_{0.5}$ films is probably due to the appearance of the the metallic Ti phase. The observation that at low fluences H and E are decreasing (Fig. 7) might be due to the fact that the relatively hard (up to 20 GPa[21]) sub-stoichiometric boron nitride is decomposed under the effect of ion bombardment. Stoichiometric films do not show such a behaviour (Fig. 8). The hardness and Young's modulus behaviour displayed in Fig. 9 for the ion-beam mixed multilayers can be understood from the GAXRD spectra of Fig. 6. The highest hardness corresponds to the appearance of the TiN phase at a fluence of 10^{16} Ar^+/cm^2.

5 CONCLUSIONS

Titanium ion implantation into boron nitride films is a suitable method to synthesize Ti–B–N coatings of variable composition. Ion-beam mixing of multilayer coatings of the type Ti/BN by argon ion bombardment generates coatings which are compositionally inhomogeneous.

The implanted films are featureless at low implantation fluences, but show many crack-like features at higher fluences due to stress-related effects. Following an annealing treatment, a self-healing effect becomes evident.

Glancing angle X-ray diffraction investigations have shown that the identified phases agree well with the prediction of the phase diagram for the system Ti–B–N.

Only relatively moderate values for H and E of about 20 and 200 GPa, in comparison to 60 and 600 GPa for Ti–B–N coatings which were synthesized by other methods, were observed.

ACKNOWLEDGEMENTS

The authors are very grateful to Dr J. Haupt (JRC-Ispra) and Dr M. Elena (IRST Trento) for their help and stimulating discussions.

REFERENCES

1. NOVOTNY, H., BENESOVSKY, F., BRUKL, C. & SCHOB, O., *Mh. Chem*, **92** (1961) 403.
2. HOLLECK, H., *J. Vac. Sci. Technol.*, **A4** (1986) 2661.
3. EMBURY, J. D. & LAHAIE, D. J., In *Mechanical Properties and Deformation Behavior of Materials Having Ultra-Fine Microstructures*, ed. M. Nastasi, D. M. Parkin & H. Gleiter. Kluwer Academic Pulishers, Dordrecht, 1993, p. 287.
4. GISSLER, W., *Surf. Coat. Technol.*, **69/69** (1994) 556.
5. PEYTAVI, J. L., LEBUGLE, A., MONTEL, G. & PASTOR, H., *High Temperature – High Pressures*, **10** (1968) 341.
6. KARNER, H., LAIMER, J., STORI, H. & RODHAMMER, P., *Surf. Coat. Technol.*, **39/40** (1989) 293.
7. MITTERER, C., RODHAMMER, P., STORI, H. & JEGLITSCH, F., *J. Vac. Sci. Technol.*, **A7** (1989) 2645.
8. KNOTEK, O., LOFFLER, F., BOHMER, M., BREIDENBACH, R. & STOßEL, C., *Surf. Coat. Technol.*, **49** (1991) 263.
9. TAMURA, M. & KUBO, H., *Surf. Coat. Technol.*, **54/55** (1992) 255.
10. MITTERER, C., RAUTER, M. & RODHAMMER, P., *Surf. Coat. Technol.*, **41** (1990) 351.
11. KNOTEK, O., BREIDENBACH, R., JUNGBLUT, F. & LOFFLER, F., *Surf. Coat. Technol.*, **43/44** (1990) 107.
12. MATTHES, B., BROSZEIT, E. & KLOSS, K. H., *Mat.-wiss. u. Werkstofftech.*, **24** (1993) 142.
13. SELBACH, E., SCHMIDT, K. & WANG, M., *Thin Solid Films*, **188** (1990) 267.
14. FRIESEN, T., HAUPT, J., GISSLER, W., BARNA, A. & BARNA, P. B., *Surf. Coat. Technol.*, **48** (1991) 169.
15. GISSLER, W., FRIESEN, T., HAUPT, J. & RICKERBY, D. G., In *Surface Engineering, Vol. 1: Fundamentals of Coatings*, ed. P. K. Datta & J. S. Gray. Cambridge, UK, 1993, p. 320.
16. FRIESEN, T., HAUPT, J., GIBSON, P. N. & GISSLER, W., In *Mechanical Properties and Deformation Behavior of Material Having Ultra-Fine Microstructures*, ed. M. Nastasi, D. M Parkin & H. Gleiter. Kluwer Academic Publishers, Dordrecht, 1993, p. 475.
17. HAMMER, P., STEINER, A., VILLA, R., GIBSON, P. N., BAKER, M., HAUPT, J. & GISSLER, W., *Surf. Coat. Technol.*, **69/69** (1994) 194.
18. GIBSON, P. N., GISSLER, W., HAUPT, J., FRIESEN, T. & FALCONE, R., *Vide, les couches minces*, **48** (1992) 297.
19. GISSLER, W., HAUPT, J., GIBSON, P. N., SASAKI, T., GUZMAN, L., ELENA, M. & MORO, L., *Surface Modification Technologies VII*, ed. T. S. Sudarshan, K. Ishizaki, M. Takata & K. Kamata. The Institute of Materials, London, 1994, p. 571.
20. DOERNER, M. F. & NIX, W. D., *J. Mater. Res.*, **1** (1992) 397.
21. GISSLER, W., HAUPT, J., CRABB, T. A., GIBSON, P. N. & RICKERBY, D. G., *Mater. Sci. Engng*, **A139** (1991) 284.
22. BUSCHERT, R. C., GIBSON, P. N., GISSLER, W., HAUPT, J. & CRABB, T. A., *J. Phys. Colloq.*, **C7** (1989) 168.